Experimental details

General

TiO_2 P25 was purchased from Degussa; methyl methacrylate (MMA, 99%), 2,2′-azobis(2-methylpropionamidine) dihydrochloride (97%), titanium (IV) isopropoxide (97%), concentrated $HClO_4$ (69% in water), concentrated HNO_3 (65% in water), acetic acid (99%) and ethylene dimethacrylate (98%), were obtained from Aldrich; ethanol (99.9%) and acetonitrile (99.9%) from Fluka. All the products were used without further purification.

PMMA particle size determination

PMMA sphere size and polydispersity were obtained with an ALV-NIBS High Performance Particle Sizer (ALV GmbH). PMMA colloidal suspensions were diluted approximately from 5 to 50-fold with Milli Q water before measurements and the particle size was extrapolated at infinite dilution.

PMMA disordered structure and PMMA opal synthesis

Monodisperse and polydisperse PMMA colloidal suspensions were loaded into 50 mL plastic falcon tubes, then centrifuged at 4300 rpm and 15°C for 30 min. The supernatant was then removed, and the PMMA disordered structure or the PMMA colloidal crystal was left to dry in air at 25°C for 24 hours.

Macroporous TiO_2 and TIO synthesis

Macroporous TiO_2 and TIO were prepared following the method proposed by Waterland and Waterhouse[1]. The interstices among PMMA spheres in PMMA disordered structure and PMMA opal were filled with a TiO_2 precursor, then the powders were calcined to remove the PMMA templates and to allow the crystallization of TiO_2. Concisely, PMMA disordered structure and PMMA opal (1.5 g) prepared by centrifugation were lightly crushed with a metal spatula to give fractured pieces of size <2 mm, which were then deposited on a filter paper (Whatman, Qualitative 1, 11μm) in a sintered glass filter funnel (Millipore). With a strong vacuum applied to the sintered glass filter funnel, a solution of TiO_2 precursor (4 mL titanium (IV) isopropoxide and 4 mL ethanol) was applied drop wise over the surface of the PMMA layer. Infiltrated samples were then left to dry in air at 25 °C for 2 h. PMMA templates were then removed by calcination in air using the following protocol; samples were ramped from 25 to 300°C at 2°C min^{-1}; held at 300°C for 5 h; then ramped from 300 to 550°C at 2°C min^{-1}; held at 550°C for 12 h; then finally allowed to cool to room temperature over 3–4 h.

Powders morphology

The morphology of the powder samples was examined by SEM (EVO-50 XVP, Zeiss). All micrographs were collected at a potential of 15 kV. Before the analysis the samples were coated by a sputtered layer of gold.

Raman spectroscopy

The crystalline phase of the powder samples was identified by Raman spectroscopy with an instrument LABRAM HRVIS (Jobin Yvon), fitted with an Olympus BX41 optical microscope. Raman spectra were excited using the 533 nm line of an Nd solid state laser. The laser power was 100 mW. Spectra were collected over the range 50–1750 cm^{-1} and at a resolution of ca. 2 cm^{-1}.

Specific surface area

Specific surface area (SSA) and porosity of the powders synthesized were measured by nitrogen adsorption using an instrument ASAP 2010 (Micromeritics Instrument Corporation). Before the analysis all the samples were outgassed at 300°C in vacuum for 24 h. Specific surface area was calculated with the B.E.T. method[2], assuming an area of 0,162 nm^2 for the N_2 adsorbed molecule. The data of the adsorption and desorption

isotherms were used to evaluate the porosity of the samples through the t-plot. The thickness of the N_2 adsorbed layer was calculated with the De Boer equation[3].

UV-Vis diffuse reflectance spectroscopy

UV−Vis diffuse reflectance spectra of the dry and wet pressed powders were obtained using an UV−Vis-NIR spectrophotometer (VG 15_DRUV_Cary 5000 DR, Varian). $BaSO_4$ was used as a reflectance standard. Spectra were registered in the 200-800 nm range at a scan rate of 150 nm min^{-1} with a step size of 1 nm; the UV source changeover was set up at 350 nm.

Irradiation procedures

The slurries were prepared by suspending in water the required amount of photocatalyst powder. Phenol aqueous solution was then added to the required amount. Experiments were run at pH 3, after adjustment with $HClO_4$.
The irradiation experiments (up to 130 min) were carried out in magnetically stirred, cylindrical Pyrex glass cells (3.5 cm diameter, 2 cm height), containing 5 mL of the aqueous suspension of the photocatalyst powder and substrate.

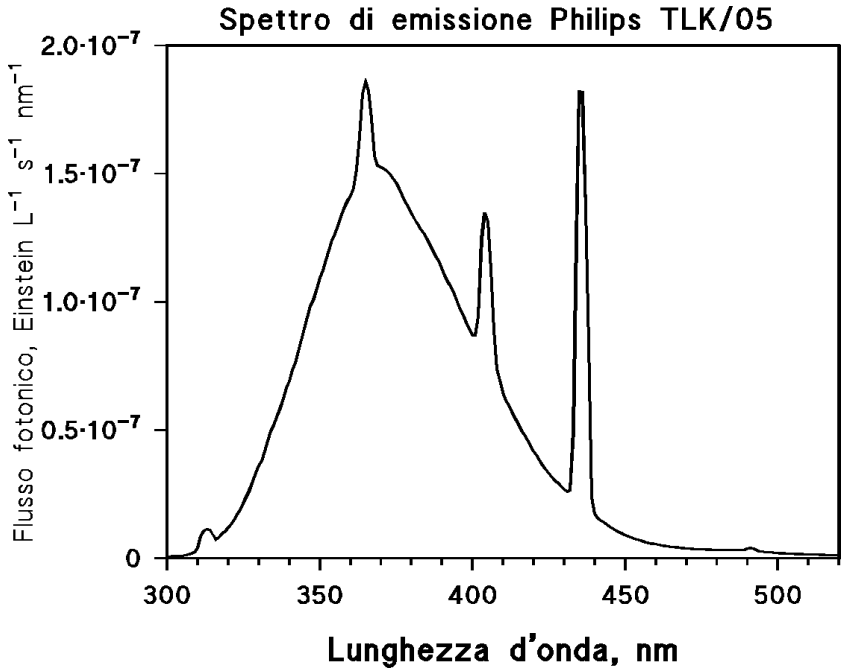

Fig. S1: Emission spectrum of a set of 5 Philips TL K05 UVA lamps

The radiation source at 365 nm was a set of five Philips TL K05 UVA lamps. The irradiance on top of the solutions was 57 W m^{-2}, measured with a CO.FO.ME.GRA. power meter. Fig. S1 reports the emission spectrum of the lamps, measured with an Ocean Optics SD2000 CCD.

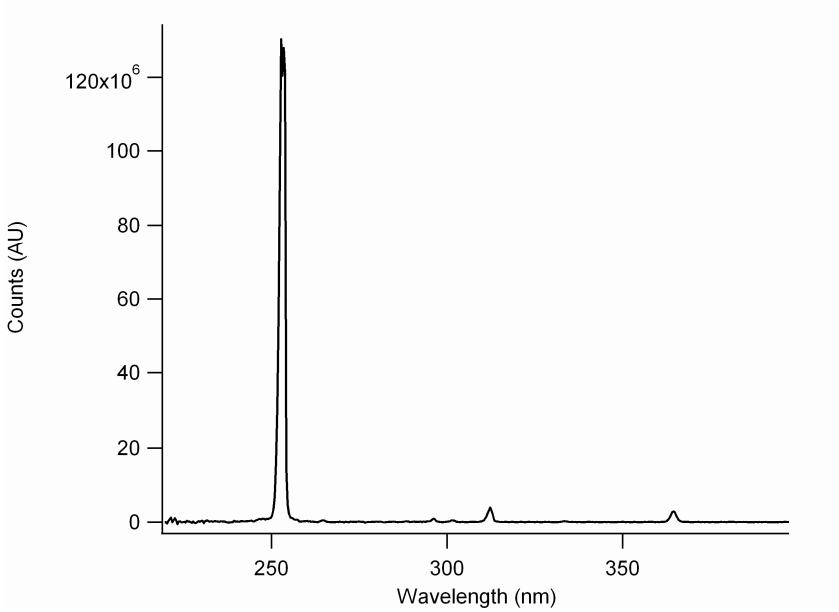

Fig. S2: Emission spectrum of a Philips TUV PL-S lamp

Irradiation at 254 nm was carried out with a Philips TUV PL-S lamp at a distance of 10 cm from the quartz cell. Fig. S2 reports the emission spectrum of the lamp, measured with an Ocean Optics SD2000 CCD. After irradiation the suspensions were filtered through a 0.45 μm filter membrane and stored at 4°C before HPLC analysis.

Supplementary results

PMMA disordered structure and PMMA opal

The centrifugation of the magnetic stirred PMMA originates a PMMA disordered structure, in which there is not periodicity, and every sphere has a different surrounding (Fig. S3). Fig. S4 shows the SEM micrograph of the centrifugated mechanical stirred PMMA. The result is a PMMA opal, characterized by a long range order: every sphere, unless defects such as vacancies, experiments the same environment.

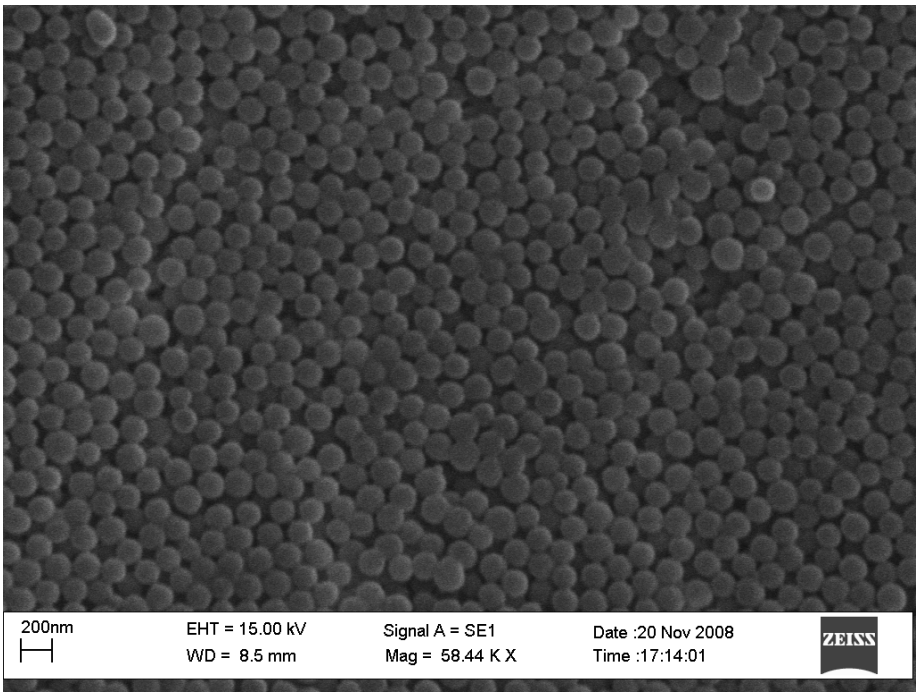

Fig. S3: SEM micrograph of the centrifugated magnetic stirred PMMA

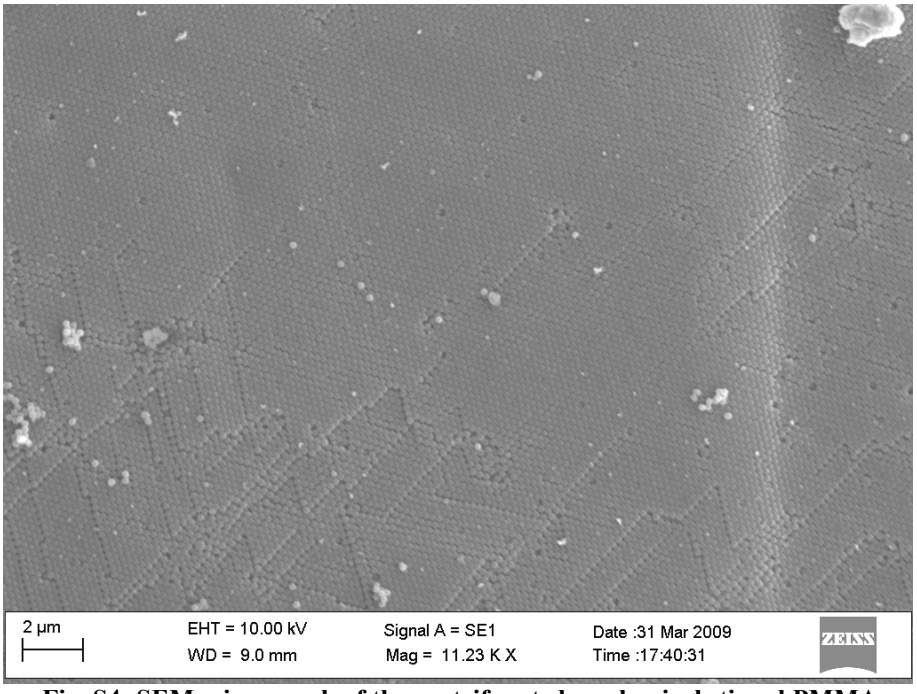

Fig. S4: SEM micrograph of the centrifugated mechanical stirred PMMA

Powders morphology

After the infiltration with TIP and ethanol and the calcining, the PMMA disordered structure originates a macroporous TiO_2 with a disordered arrangement of the pores (Fig. S5 and 1). As shown in Fig. S5 the powder is composed by big particles, also exceeding 100 µm, and by some smaller fragments.
Instead, with the same treatment, from the PMMA opal a TIO is obtained, which displays an ordered disposition of the pores (Fig. 2). As in the case of the macroporous TiO_2, also the TIO is composed by particle bigger than 100 µm and by some smaller fragments.

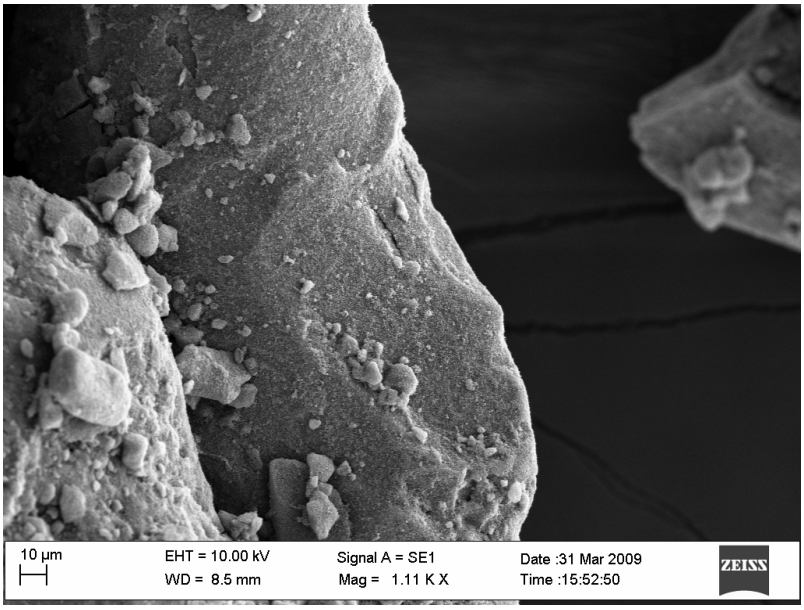

Fig. S5: SEM micrograph at low magnification of macroporous TiO_2

Raman spectroscopy

The Raman spectra (Fig. S6) of macroporous TiO_2 and TIO show that anatase is present in both samples as TiO_2 crystalline form.

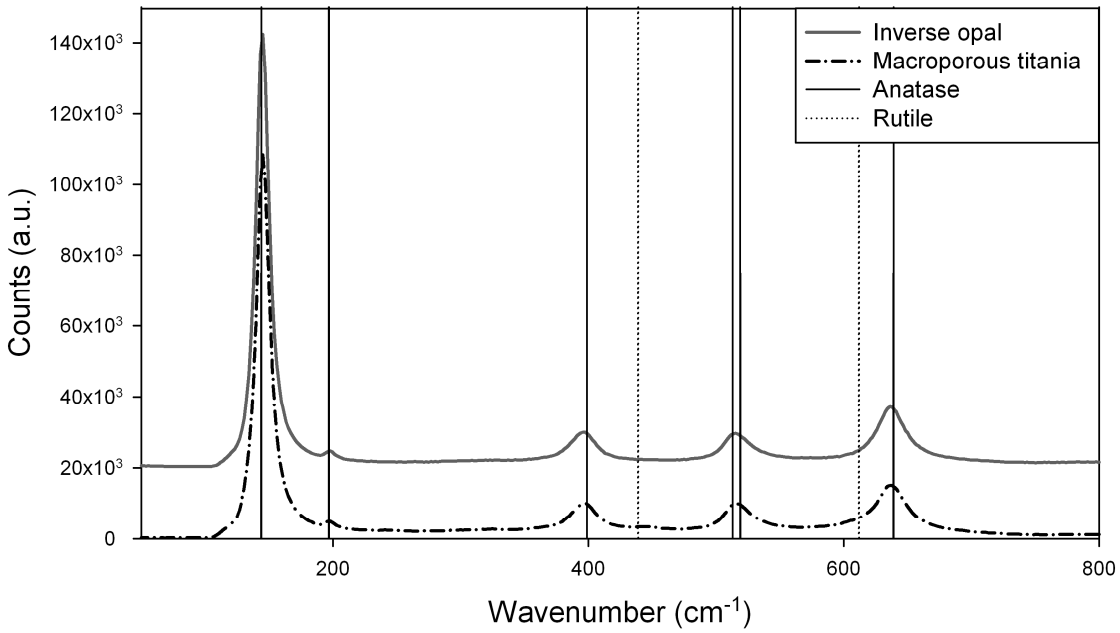

Fig. S6: Raman spectra of macroporous TiO_2 and TiO_2 inverse opal

Specific surface area

Both macroporous TiO_2 and TIO have a low SSA (respectively 28 and 18 $m^2\ g^{-1}$) and similar features in the adsorption isotherms and t-plots. The adsorption isotherms have hysteresis loops at high N_2 relative pressure, and the t-plots deviate from linearity only at high statistical thickness (> 15 Å, Fig. S7 and S8). This is coherent with the presence of macropores deriving from the polymer template; moreover macropores account for the whole porosity of the samples, because, from the analysis of the t-plots (Fig. S8), there is no evidence of the presence of micropores and mesopores.

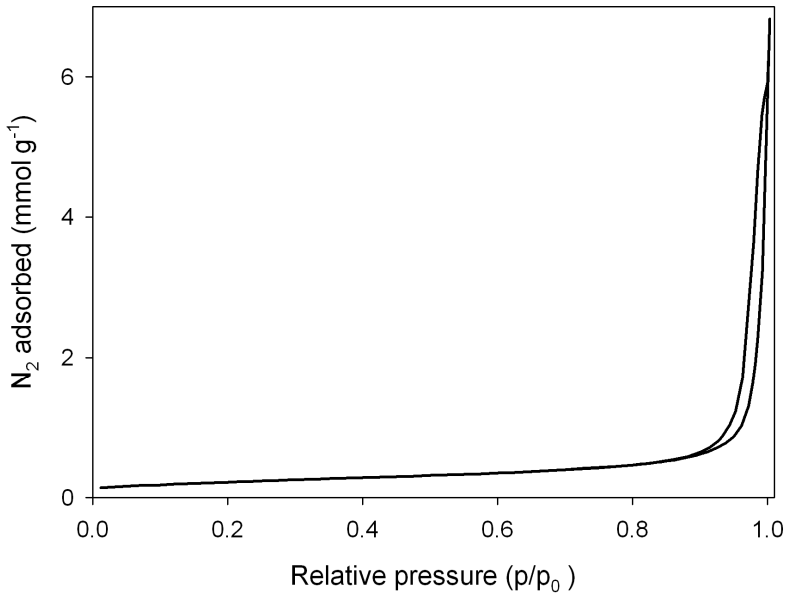

Fig. S7: Adsorption isotherm of TiO_2 inverse opal. Macroporous TiO_2 shows a similar trend

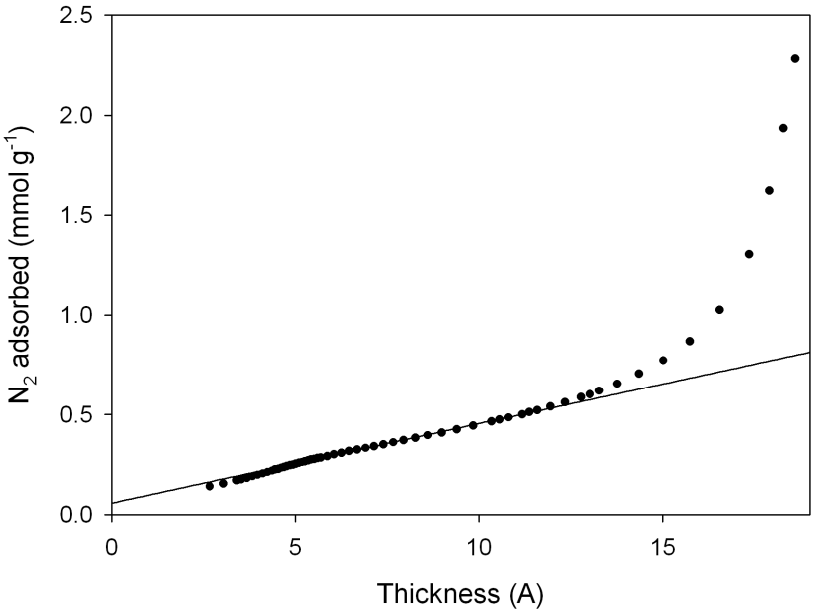

Fig. S8: t-Plot of TiO_2 inverse opal. Macroporous TiO_2 shows a similar trend

UV-Vis diffuse reflectance spectroscopy

The comparison of the reflectance spectra of macroporous TiO_2 and TIO confirms the presence of a PBG at 270-280 nm in air and 320-330 nm in water (Fig. S9 and S10 insets). The PBG is appreciable even if at those wavelengths there is a strong absorption of TiO_2.

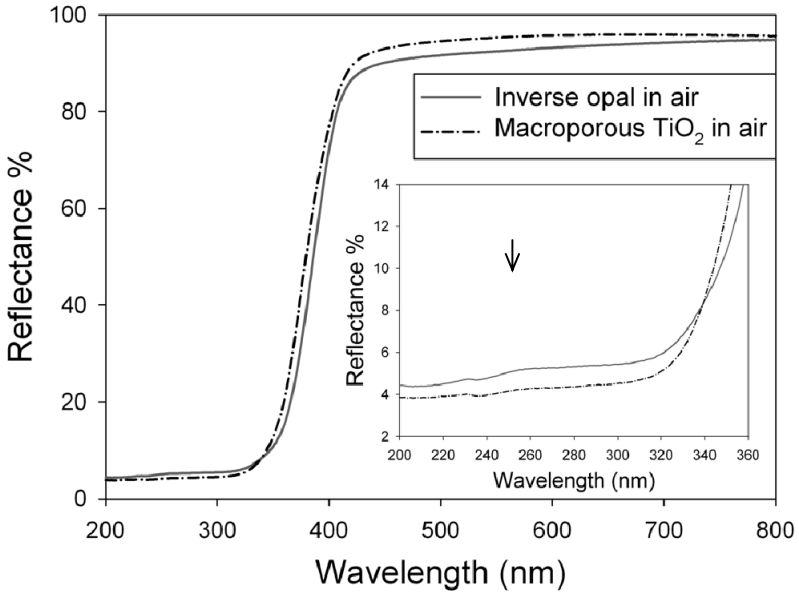

Fig. S9: UV-Vis diffuse reflectance spectra of macroporous TiO_2 and TiO_2 inverse opal in air

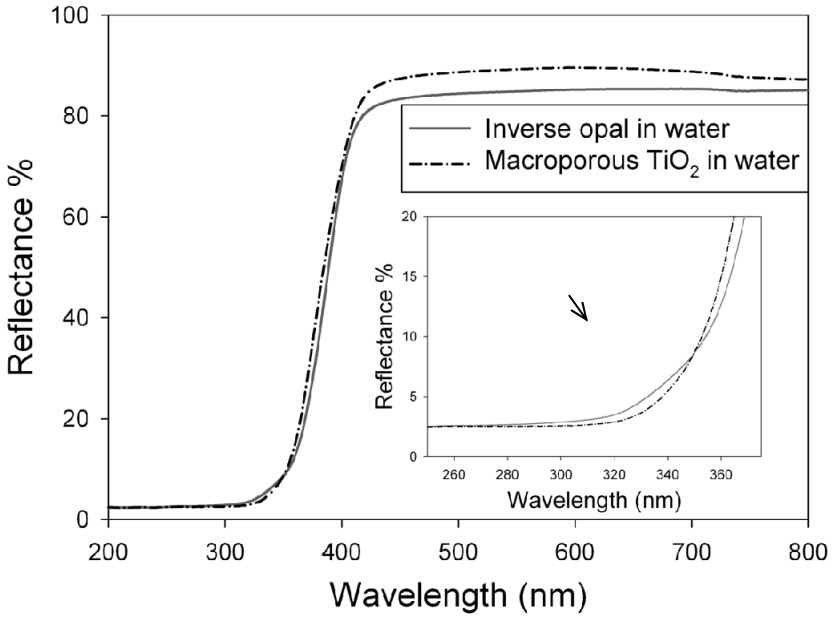

Fig. S10: UV-Vis diffuse reflectance spectra of macroporous TiO_2 and TiO_2 inverse opal in water

References

1. G. I. N. Waterhouse and M. R. Waterland, *Polyhedron*, 2007, **26**, 356.
2. S. Brunauer, P. H. Emmett and E. Teller, *J. Am. Chem. Soc.*, 1938, **60**, 309.
3. J. H. de Boer, B. C. Lippens, B. G. Linsen, J. C. P. Broekhoff, A. van den Heuvel and T. J. Osinga, *J. Colloid Interface Sci.*, 1966, **21**, 405.